qualitative and quantitative characteristics of the curves (coefficient of coincidence, analysis of characteristic years, and so forth). Those individual trees that could not be matched were rejected. The lengths of the group chronologies vary considerably, depending on the age of the specimens and the degree of overlap. The principal characteristics of each chronology are given in Table 1.

From the investigation it can be concluded that (i) at each locality several pine trees were at least partly coeval; (ii) at the edge of the bog the simultaneousness can be demonstrated over a relatively large area (D E E°), where the pine forest existed for more than three centuries; (iii) the large proportion of curves, which could not be cross-dated (24 out of 52), indicates irregular growth and cannot be considered as proof of differing ages; and (iv) in the center of the bog the groups cannot be cross-dated, undoubtedly because the sequences are not long enough and the growth too irregular. Of the two series that were relatively long (D°, 330 years, and D E E°, 369 years), samples that comprised not more that 10 ring-years each were selected at regular intervals of 50 or 30 years for radiocarbon analysis. Unfortunately, the complete range could not be spanned owing to the condition of the cores of stumps and the breadth of outermost rings. Of group D°, five samples were analyzed from stump D°1, spanning 205 years; and of group D E E°, 14 samples, spanning 284 years, were analyzed (Table 2).

When all the results obtained for each group are used, the conventional radiocarbon dating (*6*) for group D° with 330 ring-years is 7200 to 6870 years before the present (B.P.), while that for group D E E° with 369 ring-years is 6440 to 6070 years B.P. The outermost rings of the younger group thus have approximately the same age as the oldest samples of the bristlecone pine chronological sequence which has been radiocarbon-dated to approximately 6130 years B.P. (conventional) (*9*). If the bristlecone pine chronology is accepted, the actual (solar) age of the youngest sample in group D E E° corresponding to 6120 conventional radiocarbon years, is about 5100 years B.C. The D° group should be approximately 800 years older.

The C^{14} activity of each sample was corrected for variations in isotope fractionation by means of the C^{13}/C^{12} ratio (*10*) and reduced to the expected value at year 0 of the group chronology, with the use of a half-life of 5730 years. The deviation in activity from the average, a delta-equivalent, is given in the last column of Table 2 and plotted in Fig. 2.

The younger group shows no trend in the C^{14} activity over the 284-year span: the slope of the best straight line through the points is -0.6 ± 2.4 per mille per century. When this result is compared with the decrease in initial C^{14} content over the period 4000 to 3000 B.C., of 4 per mille per century (*3*), we must conclude that this rapid decrease did not take place during the three centuries covered by the group. There is, however, an indication of a short-time fluctuation in C^{14} activity during this period: the sample E° 4–6 from the years 180 to 190 on the floating scale has 1.35 percent more C^{14} than the average, which causes it to seem 110 years too young. The older series, D°1, shows an increase in the initial C^{14} content amounting to $+2.5 \pm 3.7$ per mille (best straight line) over the two centuries covered.

Although the length of the two floating chronologies is admittedly too short to gain certainty about the trend in C^{14} prior to 5000 B.C., the indications are that at about 6000 B.C. (solar years) the C^{14} content was increasing; at about 5000 B.C. the level was more or less constant, to start decreasing again after 4000 B.C.

J. C. VOGEL*
Natuurkundig Laboratorium,
University of Groningen,
Groningen, Netherlands
W. A. CASPARIE
Biologisch-Archaeologisch Instituut,
University of Groningen
A. V. MUNAUT
Laboratoire de Palynologie et
Phytosociologie, University of
Louvain, Louvain, Belgium

References and Notes

1. H. de Vries, G. W. Barendsen, H. T. Waterbolk, *Science* **127**, 129 (1958); H. de Vries and H. T. Waterbolk, *ibid.* **128**, 1550 (1958).
2. C. W. Ferguson, *ibid.* **159**, 839 (1968).
3. H. E. Suess, *J. Geophys. Res.* **70**, 5937 (1965); in *Radioactive Dating and Methods of Low-Level Counting* (Intern. Atomic Energy Agency, Vienna, 1967), p. 143.
4. ———, *Z. Phys.* **202**, 1 (1967); J. C. Vogel, *Helinium* **9**, 3 (1969).
5. A detailed investigation of the structure and genesis of this peat bog is being conducted by W. A. Casparie.
6. Age calculated with a half-life for C^{14} of 5570 years and assuming the initial C^{14} content of the samples, after correction for variations in isotope fractionation, to have been equal to 0.95 of that of the U.S. National Bureau of Standards oxalic acid C^{14} standard. B.P., before the present, that is, before A.D. 1950.
7. B. Huber, *Holz Roh Werkstoff* **6**, 263 (1943); E. Schulman, *Dendroclimatic Changes in Semiarid Arizona* (Univ. of Arizona Press, Tucson, 1956).
8. A. V. Munaut, *Agricultura* **14**, 193 and 361 (1966).
9. E. K. Ralph, H. N. Michael, *Archaeometry* **10**, 1 (1967).
10. Thanks are due to W. G. Mook for performing the C^{13} analysis.

* Present address: Natural Isotopes Division, CSIR, Pretoria, South Africa.

12 August 1969

Nonexistence of Large Mascons at Mare Marginis and Mare Orientale

Abstract. *The analysis of line-of-sight residual accelerations from Lunar Orbiters 3 and 5 does not show any evidence for large mascons near the lunar limbs. Although unfavorable geometry reduces the acceleration effect due to any mascon near the limb, simulations show that large masses at Mare Orientale and Mare Marginis would produce substantial accelerations, in complete disagreement with the actual Doppler tracking data obtained from a Lunar Orbiter experiment.*

The observation of large accelerations of Lunar Orbiter spacecraft above the ringed maria on the lunar nearside (*1*), and the association of these accelerations with mass concentrations (mascons) immediately beneath these maria (*1*), have prompted speculation that all ringed maria have associated mascons whose masses increase with increasing ring diameter. In particular, Campbell *et al.* have suggested that there are mascons at Mare Orientale and Mare Marginis which are 1.43 and 2.42 times the size of the Mare Imbrium mascon, respectively (*2*). We show here that typical Doppler tracking data, from Lunar Orbiter spacecraft passing near these features, are in complete disagreement with such an assignment of masses.

Figure 1 shows the Doppler residuals, after a least-squares estimation of the six parameters of spacecraft state at epoch, for an orbit of low inclination (21°). This orbit of Lunar Orbiter 3 traversed from west to east, across the nearside of the moon, passing over Mare Orientale and Mare Crisium and near Mare Marginis at the indicated times. For comparison, Fig. 1 also shows a simulation of the residuals which would result for a hypothetical spacecraft on the same trajectory over a spherical moon having eight mascons, with the sizes and locations postulated by Campbell *et al.* (*2*). The Doppler signatures at the regions of Mare Ori-

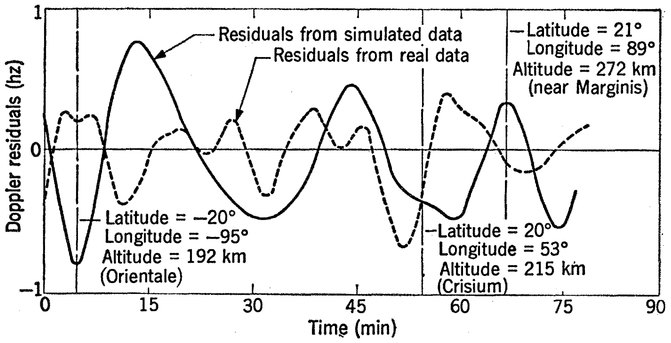

Fig. 1 (left). Real and simulated data for equatorial orbit.

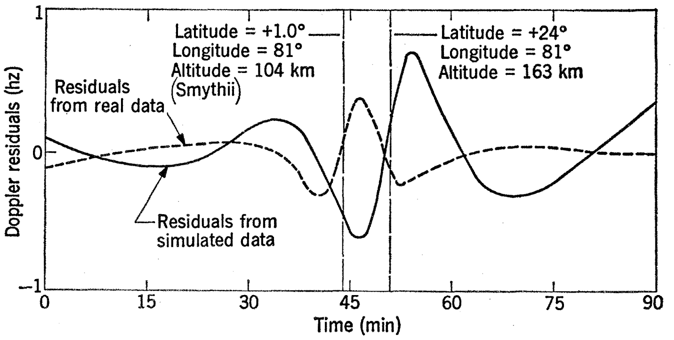

Fig. 2 (right). Real and simulated data for polar orbit.

entale and Mare Marginis are almost exactly opposite for the two curves. The following discussion of the simulated residuals will clarify the precise nature of the disagreement.

Doppler residuals provide a least-squares filtered measurement of the portion of the velocity component along the line of sight which is not predicted by simple orbital motion. The derivative of the residuals as a function of time provides a least-squares filtered measurement of the line-of-sight acceleration. The residual curve for mascons near the limb should show a line-of-sight acceleration that is zero when the spacecraft is directly over the mascon, negative when the spacecraft is beyond the mascon, and positive when the spacecraft is on the nearside (relative to the earth) of the mascon. Since the spacecraft travels from west to east, the curve over Mare Orientale should go from negative to positive (approaching from the farside) whereas near Mare Marginis it should go from positive to negative (approaching from the nearside). This expected mascon behavior is precisely what is shown by the simulated curve in Fig. 1. The spurious peaks between the simulated residuals near Mare Orientale and Mare Marginis have much smaller slopes and arise from the distorting effects of the least-squares filter. This distortion also causes the peak accelerations observed near the simulated mascons to be 30 percent too small and has been described by Gottlieb (*3*). Furthermore, the accelerations due to the Mare Crisium mascon are barely discernible in the simulated residuals (although they are the most prominent feature of the residual curve for the real data) because of the overwhelming effect of the hypothetical Mare Marginis mascon.

The curve for the actual Doppler tracking data (Fig. 1) does show a small dip directly over Mare Orientale, thus indicating a mass of 3×10^{-6} lunar mass (0.1 of the value for the Imbrium mascon) at a depth 50 km below the surface. This estimate agrees, approximately, with the value suggested by Muller and Sjogren (*4*) on the basis of data from polar orbits. Since the major features of the actual Doppler curve near Mare Orientale are exactly opposite to those of the simulated data, we conclude that the small positive region is surrounded by a large negative region; this result does not agree with the suggestion of Campbell *et al.* (*2*). (We are presently completing a consistent gravity model of the front side of the moon in which Mare Orientale is represented by a small positive region surrounded by a large negative region; an estimation of the orbit with this model reduces the residuals near Mare Orientale.)

Although the simulated curve (Fig. 1) does show the effects of a hypothetical Mare Marginis, the 21° inclination of the orbit prevented the spacecraft from coming very close to the hypothetical location of 30°N latitude; thus a more complete understanding can be obtained from an orbit with high inclination (85°). Figure 2 shows the actual residual curves from such an orbit and the curves simulated from the model of Campbell *et al.* The acceleration due to Mare Smythii is apparent in the real data, whereas the simulation shows that a mascon at Mare Marginis of the magnitude conjectured by Campbell *et al.* (*2*) would give twice as large an observed acceleration at an erroneous location. Figures 1 and 2 together show that the upper limit for any mascon at Mare Marginis must be less than 5 percent of the Mare Imbrium mascon.

These arguments are based on the assumption that the mascons are spherical. In order to estimate the magnitude of a possible surface distribution, we have used Ivory's solution for the force due to an oblate spheroid (*5*) and have taken the limit of zero thickness for the spheroid. Numerical evaluation of the horizontal force 100 km above a spheroidal disk 1000 km in diameter shows that the peak horizontal force is one-half the peak vertical force (a larger fraction than for a spherical mass). These computations also show that the mass of a disk 1000 km in diameter is about as efficient in producing accelerations as a spherical mass at a depth of 300 km, which is the depth used in our simulations. If the diameter of the disk is smaller (and 1000 km is already much too large for any gravitationally verified feature), the depth of the equivalent spherical mass will also be smaller, thus putting an even tighter upper bound on the positive masses of the two limb features.

The only mascon which we find near the limbs is at Mare Smythii. After correction for viewing geometry, the analysis of line-of-sight accelerations indicates a mass that is about 0.35 of the mass at Mare Imbrium. [Campbell *et al.* (*2*) have suggested that the Mare Marginis–Mare Smythii combination has 2.42 times the mass of the Mare Imbrium mascon.] Since the possibility of large masses on the lunar limbs is precluded, the remaining large mascons of the model of Campbell *et al.* will all lie close to the earth-moon axis. If the lunar triaxial ellipsoidal moments, determined from the physical libration data (*6*), were due to mascons, as has been suggested by O'Leary *et al.* (*7*), these remaining mascons would make the value of C_{22} (the asymmetric part of the triaxiality) approximately half the value of J_2 (the oblate portion of the triaxiality), in disagreement with the libration estimate. It would, of course, be possible to speculate on the existence of other mascons on the farside of the moon which could redress the imbalance left by the removal of Mare Orientale and Mare Marginis, but the results reported here eliminate the possibility of any presently verifiable scheme.

P. GOTTLIEB
P. M. MULLER
W. L. SJOGREN
Jet Propulsion Laboratory, California Institute of Technology, Pasadena

References and Notes

1. P. M. Muller and W. L. Sjogren, *Science* **161**, 680 (1968).
2. M. J. Campbell, B. T. O'Leary, C. Sagan, *ibid.* **164**, 1273 (1969).
3. P. Gottlieb, *Jet Propulsion Lab. Space Programs Sum. 37–55* (1969), vol. 3, p. 3.
4. P. M. Muller and W. L. Sjogren, *Proc. Comm. Space Res. 12th*, in press.
5. F. B. Moulton, *An Introduction to Celestial Mechanics* (Macmillan, New York, 1914), p. 133.
6. K. Koziel, *Trans. Int. Astron. Union* **12A**, 223 (1964).
7. B. T. O'Leary, M. J. Campbell, C. Sagan, *Science* **165**, 651 (1969).
8. We thank L. Ross for coordinating the computations for the determination of the orbits. This paper presents the results of one phase of research carried out at the Jet Propulsion Laboratory, California Institute of Technology, under NASA contract No. NAS 7-100.

28 July 1969

X-ray Diffraction Studies of Echinoderm Plates

Abstract. *X-ray diffraction studies confirm that, with few exceptions, each skeletal element of echinoderms is a single crystal of magnesium-rich calcite and that a relation exists between the shape of the element and the crystallographic* a- *and* c-*axes. The exceptions include the teeth of echinoids, and the calcareous ring as well as the anal teeth of holothurians. The tubercles of an echinoid plate begin their growth as parts of the single crystal of the plate; under the mechanical action of the spines that are attached to them, they become partly polycrystalline, as shown by scanning electron microscopy and by x-ray powder diffraction. The interface between inorganic crystalline and organic amorphous matter in the skeletal element appears to be the first example reported in nature of a periodic minimal surface.*

The echinoderm skeleton is known to be composed of magnesium-rich calcite; no aragonite has been reported, no other crystalline inorganic or organic phase is present, and even evidence for a solid amorphous phase is lacking (*1, 2*). However, there persists in the literature (*3*) confusion on the crystallographic nature of the skeletal element: Does it consist of a single crystal, subparallel crystals, or a polycrystalline aggregate? In its external shape a skeletal element, as strikingly shown recently by scanning electron microscope photographs (*4*), is completely noncrystallographic, consisting of mammillated surfaces that show neither planes nor straight edges, leave alone interfacial angles! Nevertheless, it must be crystalline if it diffracts x-rays. It is monocrystalline, that is, made up of "a single crystal," if all its parts diffract coherently to give discrete spots on the film—proof that it must be referred to a single continuous lattice. It will be polycrystalline, if its parts diffract incoherently—smearing the spots into smooth continuous powder-diffraction lines if the aggregate is finely crystalline and into gritty-looking lines if it is coarsely crystalline. The grain size, which is the size of the component crystals, can be estimated from the appearance of the diffraction lines: diffuse, sharp, "gritty," corresponding to ~ 0.1 μm or less, ~ 1 μm, and ~ 10 μm or more, respectively.

We used the precession camera (with Mo$K\alpha$ radiation), as well as the Weissenberg and back-reflection Weissenberg cameras (with Cu$K\alpha$ and Fe$K\alpha$), the powder camera (Cu$K\alpha$), the petrographic microscope, and the electron probe. The rhombohedral calcite crystal is referred to its hexagonal triple cell, [$a \sim 5$ Å, $c \sim 17$ Å, $6(\mathrm{Ca,Mg})\mathrm{CO}_3$ per cell, cleavage $\{10.4\}$]. The directions of *a* and *c* are used to describe the crystal orientation with respect to plate shape. The accuracy with which such an orientation relation can be determined is limited by the variation in the plate shape itself and by the range of orientations of the plates on the body, which can be considerable. The orientation relations we are reporting (Table 1) are accurate enough to insure that the first orientation pattern obtained on the precession camera will yield the desired crystallographic directions. In other words, perfect adjustment of these directions will not require angular corrections larger than 7° or 8°. At least three plates were tested from each species. They always agreed in *c* direction. The a directions were occasionally found to be somewhat more variable, although they too were found to be oriented when the plate offered a reference direction, be it a row of holes in a holothurian plate or the flattening of a spine in an ophiuroid. We have been warned (*5*) that generalizations based on so few samples may be hazardous; our present aim is mainly to induce more zoologists to explore this field of biocrystallography.

The study was begun with the intent of testing, by x-ray diffraction, a hypothesis proposed by Towe (*6*)—that the primary deposit of calcite in echinoid skeletal plates is polycrystalline, the shape of the deposit being thus readily adjusted to the needs of the organism. Recrystallization resulting in a single crystal would take place in the solid state as a secondary process, the shape of the polycrystalline plate being preserved. This is an intriguing proposal for the formation of a pseudomorph; it is the reverse of a process that is common in mineralogy: a single crystal transforms to, or is replaced by, another

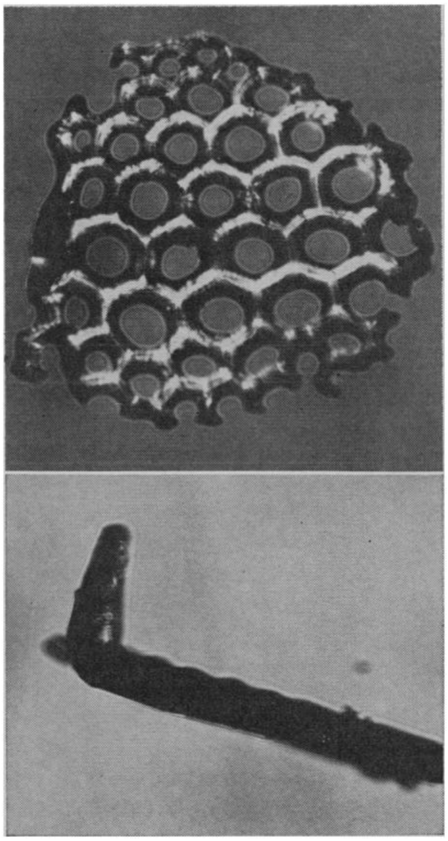

Fig. 1. (Top) Plan view of plate from holothurian *Echinocucumis hispida* (Barrett) between crossed nicols with *c* perpendicular to plane of viewing. It is imperfectly isotropic. In hexagonal net of holes, the *a* directions lie along the rows of holes. Largest horizontal width of plate: 0.42 mm. (Bottom) Profile view of the same plate showing spine at right angle to the plane of the plate. Spine and plate belong to one single crystal, at extinction between crossed nicols. Note perfect extinction: the *c* direction, along the spine axis, lies in the plane of the microscope stage.